

## Photoneutron spectrum of lead following excitation by 8999, 8533, and 8120 keV photons

J. E. McFee, W. V. Prestwich, and T. J. Kennett

*Department of Physics, McMaster University, Hamilton, Ontario, Canada L8S 4K1*

(Received 16 December 1975)

The photoneutron spectrum of natural lead has been observed for photoexcitation energies of 8999, 8533, and 8120 keV using a high-resolution  $^3\text{He}$  ionization chamber. The photons were obtained from the  $(n, \gamma)$  reaction on a nickel target positioned in a nuclear reactor. The  $Q$  values for the three reactions  $^{208}\text{Pb}(\gamma, n)^{207}\text{Pb}$ ,  $^{207}\text{Pb}(\gamma, n)^{206}\text{Pb}$ , and  $^{206}\text{Pb}(\gamma, n)^{205}\text{Pb}$  have been determined and are, respectively,  $7369 \pm 5$ ,  $6743 \pm 3$ , and  $8087 \pm 3$  keV. Neutron groups corresponding to different final states following excitation by one of the three photon components have been observed and their partial cross sections are reported. The distribution and some systematics of the neutron reduced widths have been studied. The absolute cross sections of the reaction  $^{208}\text{Pb}(\gamma, n)^{207}\text{Pb}$  at 8999 and 8533 keV photon energies have been found to be  $6.8 \pm 2.9$  and  $5.0 \pm 2.1$  mb, respectively.

[ NUCLEAR REACTIONS  $^{206, 207, 208}\text{Pb}(\gamma, n)$ ,  $E = 8.120, 8.533, 8.999$  MeV; measured  $\sigma(E; E_n)$ . Deduced  $Q$ , reduced widths. ]

### I. INTRODUCTION

Photoneutron spectroscopy is a useful tool for probing the energy states of nuclei and as such is complementary to single-neutron transfer reactions. In view of the recent discovery of collective resonances<sup>1</sup> other than the familiar giant dipole resonance, it is expected that photoneutron spectroscopy can assist in the investigation of such resonances. In addition, photoneutron spectroscopy may clarify our understanding of the photon interaction process in nuclei,<sup>2</sup> a process which is not yet fully understood.

Most  $(\gamma, n)$  experiments in the past have used photon beams of wide energy spread. The tagged-photon bremsstrahlung technique developed recently has a  $\gamma$ -ray energy dispersion of 70 keV [full width at half-maximum (fwhm)],<sup>3</sup> whereas the standard bremsstrahlung threshold or position annihilation-in-flight techniques yield typically hundreds of keV. Although much useful information can be obtained from such experiments, these large energy spreads normally restrict the investigation either to averaging over many resonances in the target nucleus or to observing transitions to only the ground state or the first one or two excited states in the residual nucleus. Monochromatic  $\gamma$ -ray sources, derived from neutron capture by a target placed in a nuclear reactor and having typical energy spreads of several eV (fwhm), have been used previously,<sup>4,5</sup> but with detection systems which provide no energy information. The highest resolution neutron spectrometers are the time-of-flight systems which have typical energy spreads of 10 keV at 1 MeV neutron energy for long flight paths. They are restricted almost

entirely to intense positron-annihilation or bremsstrahlung facilities since their efficiency and duty cycle are very low. Recently, high-resolution neutron detectors of the  $^3\text{He}$  ionization chamber type have been developed,<sup>6,7</sup> which are comparable in energy resolution to the time-of-flight method. Since these detectors can be operated with continuous beams, their duty cycle is 100% and since they can be situated very close to the target, the increase in solid angle yields a much larger efficiency than the time-of-flight method.

In the present experiment a beam of monochromatic neutron capture  $\gamma$  rays from natural nickel has been combined with a  $^3\text{He}$  ionization chamber to study photoneutron spectra.

Jackson has noted<sup>2</sup> that there is much controversy over the value of the off-resonance cross section for photoexcitation energies in  $^{208}\text{Pb}$  just above the neutron binding energy. This is due mainly to the inability of the various techniques, described by the author, to measure this cross section directly. With the present method the cross section can be measured directly whether on or off resonance, and if the interaction occurs off resonance any direct contribution to the process will be strongly enhanced with respect to compound nucleus formation. In this work the results obtained for natural lead are presented.

The isotope  $^{208}\text{Pb}$  is of theoretical interest because of its simple nuclear configuration and also because of the controversy over the new giant collective-state resonances near 9 MeV.<sup>1,8,9</sup> In addition, information about the branching ratios to low-lying states in the  $(\gamma, n)$  reaction should assist in the interpretation of results from the several bremsstrahlung threshold experiments on lead.

## II. EXPERIMENTAL FACILITY

The experimental facility is shown schematically in Fig. 1. Since the  $\gamma$  rays were to be generated by neutron capture in the source material, it was decided to place the source directly in the core of the McMaster nuclear reactor in order to obtain the highest possible neutron flux. The position chosen for the source was colinear with a beam port and located at the outer corner of the core so that it could be viewed directly. The source container is shown in Fig. 2. It consists of an outer sleeve designed to fit into a standard fuel element position (grid plug hole) and an inner sample holder. Both containers were constructed of reactor grade aluminum with water flow channels for cooling. The inner package of dimensions 5 cm  $\times$  5 cm  $\times$  18 cm was placed inside the open topped outer holder and contained the source, in this case four 2.5-cm diam  $\times$  15-cm long rods of 99.5% pure nickel.<sup>10</sup> In order to allow easy interchange of sources, the inner package was designed such that it could be removed with a standard fuel changing tool, while leaving the outer container in place. This ensured alignment of different sources and the small package was convenient for storage within the pool or for subsequent disposal. With the existing system, sources can be changed in a few minutes and stored indefinitely in the reactor pool.

The neutron capture  $\gamma$ -ray beam was collimated by a series of stepped iron rings, barytes

concrete, and lead collimators to a diameter of 2.5 cm as determined by photographic means at the target position. Neutrons were removed from the beam by two 25-cm long borated wax plugs. Although some thermal neutrons were detected at the target position, no fast neutrons were observed when the target was removed. The  $\gamma$ -ray spectrum at the target position was observed using a Ge(Li) detector and the energies and relative intensities of the major components are shown in Table I.

The absolute beam intensity was measured by observing the Compton scattered  $\gamma$  rays from a carbon target 2.45  $\pm$  0.20 cm thick and much larger in area than the beam. The  $\gamma$  rays were viewed with a lead-collimated 7.6-cm  $\times$  7.6-cm NaI(Tl) detector at a mean angle of 31.6  $\pm$  0.3  $^\circ$  with respect to the beam. All incident  $\gamma$  rays above 5.8 MeV were scattered into a single broad peak with centroid at 2.52  $\pm$  0.02 MeV. Since the photoefficiency of NaI(Tl) is well known around 2.5 MeV, the total photon flux above 5.8 MeV and the flux for the different photon components could be determined. A thermal neutron flux of approximately 10<sup>13</sup> cm<sup>-2</sup> s<sup>-1</sup> at the source position was thus found to yield a beam of (2.7  $\pm$  0.5)  $\times$  10<sup>6</sup> s<sup>-1</sup> for the 8999-keV photon at the target. The photon energy spread, primarily due to Doppler broadening (assuming a 38  $^\circ$ C nickel source temperature), was calculated to be approximately 8.4 eV at a photon energy of 8999 keV.

The neutron detector was a gridded <sup>3</sup>He ionization

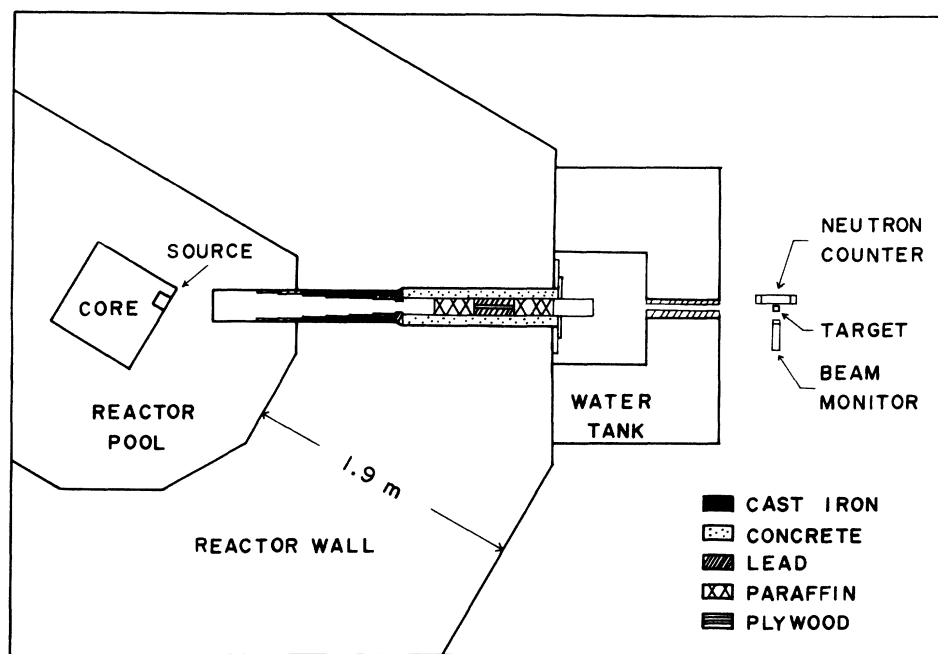


FIG. 1. Schematic view of the McMaster nuclear reactor monochromatic spectroscopy facility.

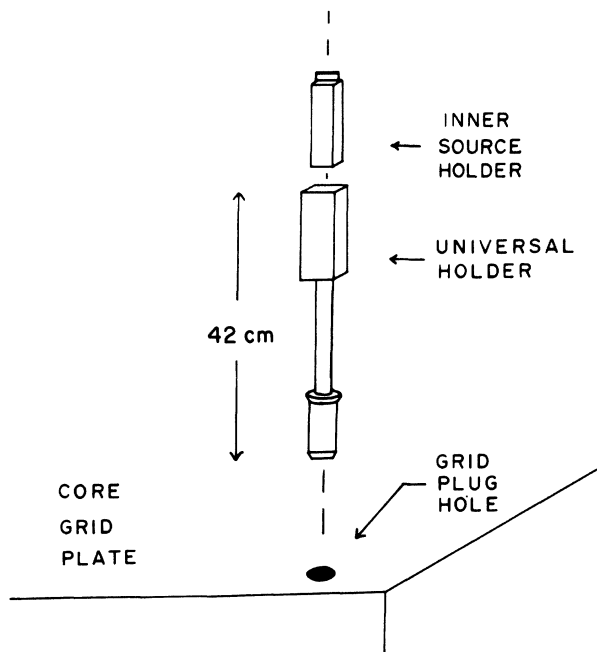


FIG. 2. Exploded view of the outer (universal) source holder and inner source holder. The nickel source material contained in the inner holder is not shown.

TABLE I. Intensities of beam photons.

Energy (MeV)	Relative intensity <sup>a</sup>	Accepted nickel intensity <sup>a,b</sup>
11.387	5.8 ± 0.5	c
8.999	1000.0 ± 8.0	1000 ± 1
8.533	434.4 ± 5.9	450 ± 1
8.120	76.7 ± 3.5	83 ± 1
7.819	215.7 ± 4.8	217 ± 1
7.724	154.3 ± 4.0	d
7.555	112.3 ± 3.8	118 ± 1 <sup>e</sup>
7.534		
6.837	284.7 ± 4.6	286 ± 1
6.584	38.1 ± 3.4	47 ± 1
6.105	49.2 ± 4.1	50 ± 1
5.974	19.0 ± 3.9	18 ± 1
5.837	75.1 ± 4.5	72 ± 1 <sup>e</sup>
5.817		

<sup>a</sup> Arbitrary units. Unless otherwise stated, lines arise from the  $^{58}\text{Ni}(n, \gamma)^{59}\text{Ni}$  reaction.

<sup>b</sup> N. C. Rasmussen, Y. Hukai, T. Inouye, and V. J. Orphan, Massachusetts Institute of Technology Report No. MITNE-85, 1967 (unpublished).

<sup>c</sup> Line arises from  $^{59}\text{Ni}(n, \gamma)^{60}\text{Ni}$  reaction and hence intensity is dependent on irradiation time.

<sup>d</sup> From  $^{27}\text{Al}(n, \gamma)^{28}\text{Al}$ .

<sup>e</sup> Total intensity of two lines which could not be resolved.

chamber<sup>11</sup> which is described in the literature.<sup>6,7</sup> The resolution of the detector was observed to vary smoothly from 13 keV at thermal to 27 keV at 1-MeV neutron energy.

In order to determine photon neutron cross sections the efficiency of the detector was required as a function of neutron energy. Although the most common method of determining the relative efficiency is by use of a monoenergetic neutron producing reaction from a charged particle accelerator, it is very difficult to reproduce the present geometry with such a system.

It was therefore decided that an alternative method would be to calculate the relative efficiency  $\eta(E)$  using the known  $^3\text{He}(n, p)^3\text{H}$  cross section  $\sigma(E)$  as a function of neutron energy<sup>12</sup> and the neutron energy-dependent proton-triton wall effect fraction  $P(E)$  calculated from the tabulated values of Batchelor and Morrison.<sup>13</sup> The efficiency, normalized to 1 MeV, was calculated using the equation:

$$\eta(E) = \frac{\sigma(E)}{\sigma(1 \text{ MeV})} \times \frac{[1 - P(E)]}{[1 - P(1 \text{ MeV})]} \quad (1)$$

The efficiency thus calculated was compared with two independent experimental efficiency measurements employing the  $^7\text{Li}(p, n)^7\text{Be}$  reaction performed on two identical  $^3\text{He}$  neutron detectors.<sup>14</sup> Although the experimental measurements were made using a different geometry, it was found that the calculated efficiency was well within the error of the experimental measurements. This was considered reasonable since the experimental errors are approximately 15% and thus the calculated efficiency was used to obtain the relative efficiency correction in this experiment.

The next task was the determination of the absolute efficiency at a specific energy. Although it should be easy in principle to measure this using an  $(\alpha, n)$  type neutron source it is, in fact, very difficult to interpret the experimental results, since for most neutron sources such as  $^{241}\text{Am-Be}$  the neutron spectral shape below 1.5 MeV is known only from theory and not from experimental measurement.<sup>15</sup> Since there is considerable disagreement between theoretical and experimental spectral shapes at higher neutron energies, the uncertainty in the neutron spectra below 1.5 MeV must be considered large. A more meaningful estimate of the absolute efficiency can be achieved through calculation. This was carried out using the average chord length of the detector, the  $^3\text{He}(n, p)^3\text{H}$  cross section at 1-MeV neutron energy, the wall effect fraction at 1 MeV, the  $^3\text{He}$  partial pressure (supplied by the detector manufacturer), and the average solid angle of the detector as viewed by the sample. The calculated efficiency at 1 MeV

was found to be  $5.6 \times 10^{-5}$ , and the efficiency curve from 100- to 2400-keV neutron energy is shown in Fig. 3.

Since the emitted neutrons are not necessarily isotropic, it is necessary to know the relative detector efficiency as a function of polar angle. It can be shown, by a solution of the parametric equations of a straight line intersecting a cylinder, that, when the  $\gamma$ -ray beam defines the  $Z$  axis the detector efficiency is independent of polar angle  $\theta$ . When one takes into account the finite sample size, the source to detector distance, and finite counter length, it is found that the efficiency is constant for  $34^\circ < \theta < 146^\circ$  and falls linearly to zero in the range  $18^\circ < \theta < 34^\circ$  and  $146^\circ < \theta < 162^\circ$ . It was thus expected that anisotropies in the neutron distributions would produce little error in calculating the cross sections. To test this, an experiment was performed with the detector placed at small forward and large backward angles. After correcting for the different solid angles, it was found that the count rates were not significantly different from those of the original experiment and that the error due to anisotropy of emission of neutrons would be much smaller than the errors quoted for the reduced widths or total cross sections.

To ensure the accuracy of the absolute cross sections it was necessary to determine the integrated photon beam intensity over the experimental time interval. To do this, a beam monitor was employed which was positioned at  $90^\circ$  to the beam direction and which observed the lead target. Detection was achieved with a 3.8-cm  $\times$  3.8-cm NaI(Tl) integral mount detector shielded on all

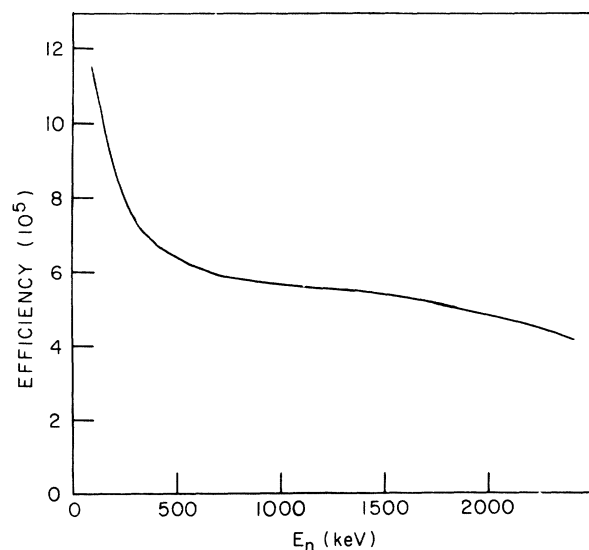


FIG. 3. Efficiency of the  $^3\text{He}$  neutron detector as a function of neutron energy.

sides with 10 cm of lead and collimated to look at only the target. A window was set at 511 keV since this is the energy of both Compton scattered photons and annihilation radiation. It was found that background was negligible and that after correcting for reactor shutdown times, the beam strength differed at most by only 4% from day to day over a four week period.

In the present experiment a 190-g sample of natural lead was used as a target and the resulting neutron pulse-height spectrum was encoded by a Nuclear Data 3300 multichannel analyzer, and analyzed using the McMaster CDC 6400 computer.

### III. RESULTS AND ANALYSIS

The photoneutron spectrum obtained, after a 1-week acquisition time, is shown in Fig. 4, and the neutron groups, their energies, relative intensities, and possible components are presented in Table II. The energies of the various groups were established by a method previously used by the authors<sup>16</sup> in the analysis of  $^{209}\text{Bi}$ . The energies of the neutron groups were calibrated first using a precision linear pulser and the intense thermal neutron group whose energy was defined by the known  $^3\text{He}(n, p)^3\text{H}$   $Q$  value.<sup>17</sup> The group centroids and areas associated with the spectrum for lead were determined by a non-linear fitting program employing an exponential tailed Gaussian as the response function. Then a linear least squares fit was done to the group centroids using the thermal neutron group and the excitation energies of lead<sup>18-20</sup> corrected for nuclear recoil to determine the energy gain and energy intercept parameter.

Finally the various experimental neutron group energies and the known values for the excitation energies of  $^{207}\text{Pb}$ ,  $^{206}\text{Pb}$ , and  $^{205}\text{Pb}$  were used to obtain the  $Q$  values for the three reactions  $^{208}\text{Pb}(\gamma, n)^{207}\text{Pb}$ ,  $^{207}\text{Pb}(\gamma, n)^{206}\text{Pb}$ , and  $^{206}\text{Pb}(\gamma, n)^{205}\text{Pb}$ . The  $Q$  values are shown in Table III together with the most recent values in the literature. The  $Q$  values for the reactions  $^{208}\text{Pb}(\gamma, n)^{207}\text{Pb}$  and  $^{207}\text{Pb}(\gamma, n)^{206}\text{Pb}$  are seen to be in good agreement with the values from the literature.<sup>17</sup> The  $Q$  value for the reaction  $^{206}\text{Pb}(\gamma, n)^{205}\text{Pb}$  is seen to be 6 keV higher than the currently accepted value but within error bars. All  $Q$  values are of comparable precision to those in the literature.

All groups were seen to correspond, after correction for nuclear recoil, to within 5-keV standard deviation to one or more existing states in  $^{207}\text{Pb}$ ,  $^{206}\text{Pb}$ , and  $^{205}\text{Pb}$  with one exception. This group occurred at neutron energy  $587 \pm 5$  keV and could not be assigned to any state in any of the lead isotopes populated by the incident  $\gamma$  rays.

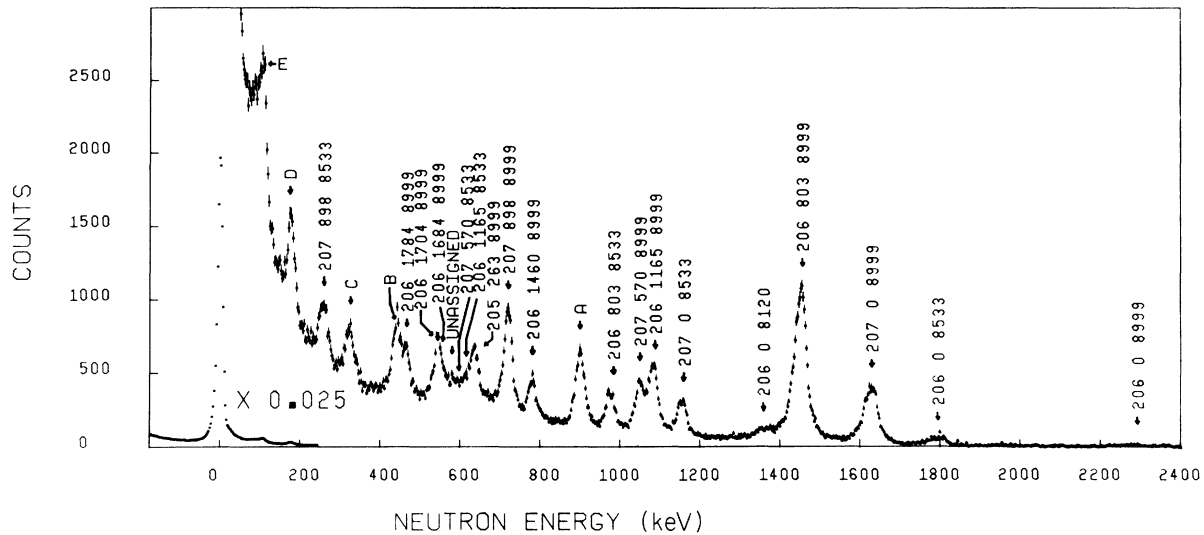


FIG. 4. The photoneutron spectrum of natural lead. Neutron groups are identified by three numbers—the isotopic number of the residual nucleus, the energy in keV of the residual nuclear state, and the energy in keV of the exciting photon. The groups labeled A through E consist of two or more components as explained in the text. The peak due to thermalized neutrons is reduced by a factor of 0.025.

This may correspond to a previously unknown state in one of the isotopes 207, 206, or 205.

To examine the neutron intensities, it is desirable to remove the energy-dependent factor arising from the neutron penetration probability through the centrifugal barrier. For an *s*-wave neutron this probability is given by<sup>21</sup>:

$$P_0 = \rho = ka, \quad (2)$$

where  $k$  is the neutron wave number and  $a$  is the nuclear radius.

For <sup>205</sup>Pb, <sup>206</sup>Pb, and <sup>207</sup>Pb residual nuclei the penetrability is given by

$$\rho \approx 1.8 \sqrt{E_n}, \quad (3)$$

where  $E_n$  is the neutron energy in MeV. Thus the measured groups can be readily made independent of energy if the neutrons emitted can be characterized as *s*-wave. Unfortunately in a portion of the neutron energy region of interest, the neutron transmission coefficients<sup>22</sup> suggest that significant contribution by *p*- and *d*-wave emission is possible. Their penetrabilities are, respectively, given by

$$P_1 = \rho^3 / (\rho^2 + 1), \quad p \text{ wave}, \quad (4)$$

$$P_2 = \rho^5 / (\rho^4 + 3\rho^2 + 9), \quad d \text{ wave}$$

and thus division by  $\sqrt{E_n}$  would not completely remove the energy dependence. For neutron energies below approximately 700 keV the neutron transmission coefficients significantly favor

*s*-wave neutrons over *d* wave. Thus if the photon interaction were pure *E1*, one could use the *s*-wave penetrability to achieve energy independence in this neutron energy range. There is, however, a possibility of an *E1-E2*<sup>1,9</sup> admixture in which case *p*-wave neutrons, which compete strongly with *s*-wave neutrons above 200 keV, can occur. Since the *E2* admixture if present is presumably small,<sup>8,9</sup> we shall, in order to simplify analysis, assume that the photon interaction is pure *E1*. If one assumes as a crude approximation an *s-d* admixture whose fractions of *s*- and *d*-wave neutrons are given by the ratio of the respective transmission coefficients and if one then attempts to achieve energy independence through division by  $P_0$ , then the maximum error over the neutron energy range of interest is 27%. In light of the above considerations it was decided to divide the intensities by  $P_0$  where *s*- and *d*-wave neutron admixtures were possible for an *E1* interaction and by  $P_2$  where only *d*-wave neutron admixtures were possible. A plot of these reduced intensities designated "reduced widths," versus neutron energy was made which indeed showed that there were no gross trends with neutron energy and it was thus felt reasonable that the reduced widths were, at least for qualitative discussion, independent of neutron energy.

In Table IV the neutron groups are classified according to the energy of the excitation photons and the energies of the states of the residual nuclei which are populated. The experimental neutron

TABLE II. Observed neutron groups.

Neutron energy (keV $\pm$ 5)	Possible components			Relative intensity ( $\pm$ 10 %)
	Residual lead nucleus	Residual nuclear state (keV)	Photon energy (keV)	
2256 <sup>a</sup>	206	0	8999	6
1780	206	0	8533	12
1615	207	0	8999	100
1446	206	803	8999	225
1370 <sup>a</sup>	206	0	8120	6
1159	207	0	8533	30
1087	206	1165	8999	60
	206	0	7819	
1054	207	570	8999	42
982	206	803	8533	27
	206	0	7724	
908	206	1341	8999	76
	205	0	8999	
	205	3	8999	
789	206	1460	8999	26
727	207	898	8999	79
643	205	263	8999	35
619	206	1165	8533	8
601	207	570	8533	5
587	...	...	...	5
573	206	1684	8999	6
	206	803	8120	
551	206	1703	8999	41
473	206	1784	8999	24
446	207	0	7819	65
	206	1341	8533	
	205	0	8533	
	205	3	8533	
330	205	576	8999	44
	206	1460	8533	
263	207	898	8533	37
	206	1998	8999	
181	207	0	7555	38
	205	263	8533	
	207	570	8120	
	206	803	7724	
110	205	803	8999	61
	206	2149	8999	
	206	1684	8533	

<sup>a</sup> Accurate to only 15 keV.TABLE III. ( $\gamma, n$ )  $Q$  values of lead isotopes.

Reaction	Present experiment (keV)	Accepted values <sup>a</sup> (keV)
$^{208}\text{Pb}(\gamma, n)^{207}\text{Pb}$	$7369 \pm 5$	$7368.2 \pm 1.4$
$^{207}\text{Pb}(\gamma, n)^{206}\text{Pb}$	$6743 \pm 3$	$6740.7 \pm 1.4$
$^{206}\text{Pb}(\gamma, n)^{205}\text{Pb}$	$8087 \pm 3$	$8081.0 \pm 3.5$

<sup>a</sup> Reference 17.

group lab energies, their relative intensities (normalized to the same isotopic abundance and photon intensity), and their partial cross sections are also presented in this table. Some groups which consist of two or more non-negligible components that cannot be resolved, have been labeled with a common letter A through E in Table IV.

It can be seen that some of the possible components of neutron groups in Table III do not appear in Table IV. A simple calculation of the relative component intensities was performed assuming that intensities were proportional to the isotopic abundance, incident photon flux, and the neutron penetrability (using the lowest possible  $l$  value). The calculations showed that some components should be of negligible intensity because of the low flux for the particular exciting photon or because of a low probability for transmission of the neutrons through the centrifugal barrier. It was noted that eight neutron groups which were calculated to be of very low intensity compared to surrounding groups, but which were capable of being resolved, were not observed. Thus although our simple calculation was considered to be too naïve to predict accurately the relative intensities of the neutron groups, it was felt to be adequate to determine which unresolved components could be neglected. Based on the above assumptions, it can be seen that the entire spectrum, with two exceptions, consists of neutrons following excitation of  $^{208}\text{Pb}$ ,  $^{207}\text{Pb}$ , or  $^{206}\text{Pb}$  target nuclei by either 8999- or 8533-keV photons. In addition, one group corresponding to an 8120-keV photoexcitation is observed as well as a group which may have components corresponding to 8120-, 7724-, and 7555-keV photoexcitations.

#### IV. DISCUSSION

In Fig. 5 the neutron reduced widths, corrected for isotopic abundance and  $\gamma$ -ray intensity, are plotted against the excitation energy of the residual nuclei. The neutron reduced widths, together with the spectroscopic factors for the ( $p, d$ ) and ( $d, t$ ) reactions on the three lead isotopes are tabulated in Table V.

Although the pair of neutron reduced widths associated with population of the ground state and first excited state of  $^{206}\text{Pb}$  by an 8999-keV photon exhibit large deviations from the average, it is apparent that the remainder of the reduced widths do not differ greatly from one another. The former fluctuations may be due to interference arising from an  $s$ - and  $d$ -wave neutron admixture in the population of the residual nuclear states. The possibility of  $s$ - $d$  interference is further

TABLE IV. Low-lying states in  $^{207}\text{Pb}$ ,  $^{206}\text{Pb}$ , and  $^{205}\text{Pb}$ .

Residual isotope	$E_\gamma$ (keV)	$E_x$ (keV)	$J^\pi$	Observed neutron energy (lab) (keV $\pm$ 5)	Relative <sup>a</sup> intensity ( $\pm$ 10 %)	$\sigma_{\gamma n}$ <sup>b</sup> (mb)	
207	8999	0 <sup>c</sup>	$\frac{1}{2}^-$	1615	100	3.1	
		570	$\frac{5}{2}^-$	1054	42	1.3	
		898	$\frac{3}{2}^-$	727	79	2.4	
	8533	0	$\frac{1}{2}^-$	1159	66	2.1	
		570	$\frac{5}{2}^-$	601	12	0.4	
		898	$\frac{3}{2}^-$	263	81	2.5	
	206	8999	0 <sup>d</sup>	0 <sup>+</sup>	2256 <sup>e</sup>	19	0.6
			803	2 <sup>+</sup>	1446	556	17.2
			1165( $\pm$ 10)	0 <sup>+</sup>	1087	148	4.6
1460			2 <sup>+</sup>	789	65	2.0	
1684			4 <sup>+</sup>	573	15	0.5	
1704( $\pm$ 1)			1 <sup>+</sup>	551	102	3.2	
1784( $\pm$ 2)			2 <sup>+</sup>	473	59	1.8	
8533		0	0 <sup>+</sup>	1780	69	2.1	
		803	2 <sup>+</sup>	982	147	4.5	
		1165( $\pm$ 10)	0 <sup>+</sup>	619	45	1.4	
		1704( $\pm$ 1)	1 <sup>+</sup>	...	0	0.0	
8120	0	0 <sup>+</sup>	1370 <sup>e</sup>	181	5.6		
205	8999	263 <sup>f</sup>	$\frac{3}{2}^-$	643	74	2.3	
Unresolved groups							
A 206	8999	1340	3 <sup>+</sup>	908	76		
205	8999	0	$\frac{5}{2}^-$				
205	8999	2	$\frac{1}{2}^-$				
B 206	8533	1340	3 <sup>+</sup>	446	65		
205	8533	0	$\frac{5}{2}^-$				
205	8533	2	$\frac{1}{2}^-$				
C 205	8999	576	$\frac{3}{2}^-$	330	44		
206	8533	1460	2 <sup>+</sup>				
D 205	8533	263	$\frac{3}{2}^-$	181	37		
207	8120	570	$\frac{5}{2}^-$				
206	7724	803	2 <sup>+</sup>				
207	7555	0	$\frac{1}{2}^-$				
E 206	8999	2150( $\pm$ 1)	2 <sup>+</sup>	110	61		
205	8999	803	$(\frac{1}{2}^-, \frac{3}{2}^-)$				
Unassigned group							
...	...	...	...	587	5		

<sup>a</sup> Arbitrary normalization corrected for isotopic abundance and photon yield. Unresolved group intensities have no isotopic abundance or photon yield correction and are merely quoted relative to the group corresponding to population of the  $^{207}\text{Pb}$  ground state following 8999-keV photoexcitation.

<sup>b</sup> Relative error 10 %, absolute error 45 %.

<sup>c</sup> Reference 18.

<sup>d</sup> Reference 19.

<sup>e</sup> Centroid accurate to only 15 keV.

<sup>f</sup> Reference 20.

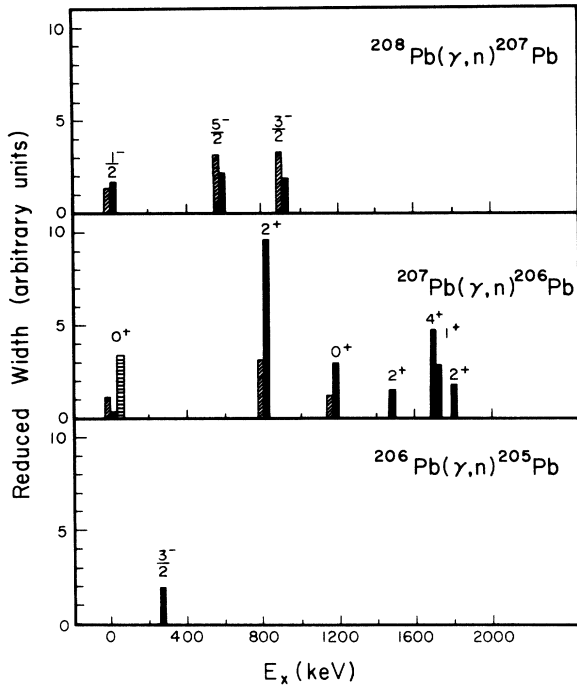


FIG. 5. Neutron reduced widths as a function of excitation energy of the residual nucleus. Solid bars correspond to excitation by an 8999-keV photon; diagonally shaded bars correspond to excitation by an 8533-keV photon and the horizontally shaded bar corresponds to excitation by an 8120-keV photon. Unresolved groups, as explained in the text, are not shown. Numbers above bars indicate the spin and parity of the residual nuclear state.

suggested by the group corresponding to the 1704-keV state in  $^{206}\text{Pb}$  which is populated at 8999 keV photoexcitation but is not seen to be populated at 8533 keV.

It is seen from the  $^{208}\text{Pb}(\gamma, n)^{207}\text{Pb}$  reaction that the total strengths at 8999 and 8533 keV are approximately equal. Because of the unresolved groups, however, it is not possible to determine if this is true for the  $^{207}\text{Pb}(\gamma, n)^{206}\text{Pb}$  and  $^{206}\text{Pb}(\gamma, n)^{205}\text{Pb}$  reactions.

The relatively small fluctuation among the neutron reduced widths is suggestive of the presence of a multichannel process. In order to test the distribution of reduced widths, each was normalized by dividing it by the mean width found for the isotope to which it corresponded. An integral frequency histogram of the reduced widths was obtained and analyzed to determine the nature of the distribution. This curve was seen to correspond closely to a  $\chi^2$  distribution of approximately 3 degrees of freedom. This hypothesis was tested by using the formulas for the unbiased estimate of the number of degrees of freedom,

$\nu$ , of a sample from a  $\chi^2$  distribution.<sup>23</sup> It was found that the estimate of  $\nu$  varied from approximately 3 when all widths were included to approximately 7 when the three widths suspected of strong  $s$ - $d$  interference were omitted. Thus, it is suggested that the observed reaction proceeds via a multichannel compound process, such as on the summed tails of resonances, or via a direct capture.

Examination of Table V reveals that the neutron reduced widths for the  $^{208}\text{Pb}$  target are somewhat correlated with the  $(p, d)$  and  $(d, t)$  spectroscopic factors, whereas the widths for the  $^{207}\text{Pb}$  target are not. A correlation, which occurs in the case of  $^{208}\text{Pb}$ , suggests that a direct or semidirect component may exist for the photon interaction process but, on the other hand, because of the ambiguity in the intermediate spin of the  $^{207}\text{Pb}$  reaction, the lack of correlation in this case does not rule out such a direct process.

Whereas only upper and lower bounds to the  $^{207}\text{Pb}(\gamma, n)^{206}\text{Pb}$  and  $^{206}\text{Pb}(\gamma, n)^{205}\text{Pb}$  reaction cross sections could be determined, due to the unresolved groups discussed earlier, the cross section for the  $^{208}\text{Pb}(\gamma, n)^{207}\text{Pb}$  reaction was found to be  $6.8 \pm 2.9$  mb at 8999-keV photon energy and  $5.0 \pm 2.1$  mb at 8533-keV photon energy. It is of interest to note that this is smaller than the cross section of  $22.6 \pm 11.3$  mb at 9.00 MeV quoted by Hurst and Donahue<sup>5</sup> and that this may be due to the indirect method employed by those authors to count fast neutrons and by the need for them to unravel the contributions from the different  $\gamma$ -ray components for a given  $\gamma$ -ray source. Although there is some confusion over what the actual value for the non-resonant cross section near threshold is,<sup>2</sup> our experimental cross sections are within the range of values quoted and are, in fact, at least a factor of 5 less than the smallest peak resonant cross sections for photon energies near 8 MeV.<sup>24</sup> Thus the narrow distribution of neutron reduced widths, the apparent correlation between the reduced widths and spectroscopic factors for the  $^{208}\text{Pb}(\gamma, n)^{207}\text{Pb}$  reaction, and the small cross section for the same reaction are all indicative of an off-resonance photon interaction. This hypothesis is strengthened by the fact that the probabilities of an interaction on resonance, calculated from the  $s$ -wave neutron strength functions,<sup>25</sup> are approximately 0.02 and 0.16 for 8999-keV photons on  $^{207}\text{Pb}$  and  $^{206}\text{Pb}$ , respectively.

For completeness, the upper and lower bounds to the cross sections for the  $^{207}\text{Pb}(\gamma, n)^{206}\text{Pb}$  and  $^{206}\text{Pb}(\gamma, n)^{205}\text{Pb}$  reactions at 8999-, 8533-, and 8120-keV photon energy have been included with the cross sections for the  $^{208}\text{Pb}(\gamma, n)^{207}\text{Pb}$  reaction in Table VI. It should be noted that our



TABLE V. Reduced widths contrasted with spectroscopic factors.

Residual nucleus	$E_x$ (keV)	$J^\pi$	$l_n^a$ E1 E2		Neutron Reduced Widths			Spectroscopic factors	
					$E_\gamma = 8999$ keV	$E_\gamma = 8533$ keV ( $\pm 27\%$ )	$E_\gamma = 8120$ keV	$C^2S/(2J+1)$ ( $p, d$ ) ( $d, t$ )	
$^{207}\text{Pb}$	0	$\frac{1}{2}^-$	0	1	163	128		b	b
	570	$\frac{5}{2}^-$	2	1	210	309		0.72	0.71
	898	$\frac{3}{2}^-$	0	1	191	327		0.90 <sup>c</sup>	0.97 <sup>c</sup>
$^{206}\text{Pb}$	0	$0^+$	0	1	26	107	321	d	...
	803	$2^+$	0	1	959	308		0.38	...
	1165	$0^+$	0	1	294	118		0.11	...
	1460	$2^+$	0	1	152	e		0.19	...
	1684	$4^+$	2	1	474	e		0.38	...
	1704	$1^+$	0	1	285	0		0.02 <sup>c</sup>	...
	1784	$2^+$	0	1	178	e		0.38	...
$^{205}\text{Pb}$	263	$\frac{3}{2}^-$	0	1	190	e		0.07	...

<sup>a</sup> Minimum possible neutron angular momentum for a given photon multipolarity.

<sup>b</sup> Reference 18.

<sup>c</sup> Spectroscopic factor for  $l_n=3$ . All others are  $l_n=1$ .

<sup>d</sup> W. A. Lanford and G. M. Crawley, Phys. Rev. C **9**, 646 (1974).

<sup>e</sup> May exist but cannot be resolved from neighboring components.

<sup>f</sup> K. Yagi, T. Ishimatsu, Y. Ishizaki, and Y. Saji, Nucl. Phys. A **110**, 41 (1968).

<sup>g</sup> R. Tickle and J. Bardwick, Phys. Rev. **178**, 2006 (1969).

limits for the  $^{206}\text{Pb}(\gamma, n)^{205}\text{Pb}$  reaction cross section at 8999-keV photon energy are lower than the 34.3-mb upper bound of Hurst and Donahue.<sup>5</sup> It is interesting that the odd- $A$  target,  $^{207}\text{Pb}$ , has a  $(\gamma, n)$  cross section which is at least a factor of 2 greater than the even- $A$  targets at equivalent photon energies.

## V. SUMMARY AND CONCLUSIONS

The photoneutron spectrum of natural lead has been observed at 8999-, 8533-, and 8120-keV photon energies by employing a high resolution  $^3\text{He}$  ionization chamber and a beam of nickel neutron capture rays from a nuclear reactor. The  $Q$  values for the three reactions  $^{208}\text{Pb}(\gamma, n)^{207}\text{Pb}$ ,

$^{207}\text{Pb}(\gamma, n)^{206}\text{Pb}$ , and  $^{206}\text{Pb}(\gamma, n)^{205}\text{Pb}$  have been determined and, although the first two  $Q$  values are in good agreement with the literature, the third is found to be  $\sim 6$  keV lower than the latest published value.

With the exception of three neutron groups, the neutron reduced widths were found to exhibit only small fluctuations, consistent with a  $\chi^2$  distribution of  $\nu \geq 3$ . The widths were found to have some correlation with the  $(p, d)$  and  $(d, t)$  spectroscopic factors for the  $^{208}\text{Pb}$  target but no correlation was found to exist for the  $^{207}\text{Pb}$  target. The cross section for the reaction  $^{208}\text{Pb}(\gamma, n)^{207}\text{Pb}$  was found to be  $6.8 \pm 2.9$  mb at 8999 keV and  $5.0 \pm 2.1$  mb at 8533-keV photon energy. Limits to the cross sections for the reactions  $^{207}\text{Pb}(\gamma, n)^{206}\text{Pb}$  and

TABLE VI. Absolute photoneutron cross sections.

Target isotope	Photon energy (keV)	Cross section <sup>a</sup> (mb)	Lower bound <sup>a</sup> (mb)	Upper bound <sup>a</sup> (mb)
208	8999	6.8	...	...
	8533	5.0	...	...
207	8999	...	29.9	40.1
	8533	...	8.0	26.8
	8120	...	5.6	...
206	8999	...	2.3	14.0
	8533	...	0	15.1

<sup>a</sup> 10% relative error; 45% absolute error.

$^{206}\text{Pb}(\gamma, n)^{205}\text{Pb}$  were found and it was observed that the cross section for the odd- $A$  target was at least a factor of 2 greater than the two even- $A$  target cross sections. These cross sections are a factor of 5 to 300 lower than the peak resonant cross sections and a factor of 10 lower than photoneutron cross sections reported from bremsstrahlung experiments at these photon energies. The latter is to be expected since the bremsstrahlung experiments average over the resonant and nonresonant regions of the target nucleus.

The small cross sections, narrow distribution of widths, and correlation with the spectroscopic factors for the  $^{206}\text{Pb}$  target suggest that the photon interaction at 8999 and 8533 keV takes place off resonance but on the sums of tails of resonances or alternatively is a direct or semidirect process.

These hypotheses are strengthened by the fact that the probability of resonance interaction in  $^{208}\text{Pb}$ ,  $^{207}\text{Pb}$ , or  $^{206}\text{Pb}$  is, as previously stated, small in this experiment.

If separated isotopes were available it would be possible to determine the total photoneutron cross sections for  $^{207}\text{Pb}$  and  $^{206}\text{Pb}$  unambiguously, by allowing certain unresolved groups to be separated into their components. It can be seen that much more information could be obtained from such an experiment.

#### ACKNOWLEDGMENTS

The authors wish to thank the National Research Council of Canada for their continued support. We are also indebted to the staff of the McMaster nuclear reactor for their assistance.

<sup>1</sup>F. R. Buskirk, H. Graf, R. Pitthan, H. Theissen, O. Titze, and Th. Walcher, *Phys. Rev. Lett.* **42B**, 194 (1972).

<sup>2</sup>H. E. Jackson, *Phys. Rev. C* **9**, 1148 (1974).

<sup>3</sup>P. A. Russo, P. A. Dickey, J. R. Calarco, and P. Axel, in *Proceedings of the Spring Meeting of the American Physical Society*, Washington, 1975 (unpublished).

<sup>4</sup>L. Green and D. J. Donahue, *Phys. Rev.* **135**, B701 (1964).

<sup>5</sup>R. R. Hurst and D. J. Donahue, *Nucl. Phys.* **A91**, 365 (1967).

<sup>6</sup>J. M. Cuttler, S. Shalev, and Y. Dagan, *Trans. Am. Nucl. Soc.* **12**, 63 (1962).

<sup>7</sup>S. Shalev, J. M. Cuttler, and Y. Dagan, in *Proceedings of the Conference on Nuclear Structure Study with Neutrons, Budapest, 1972*, edited by J. Erö and J. Szücs (Plenum, New York, 1974).

<sup>8</sup>A. Veyssiere, H. Beil, R. Bergere, P. Carlos, and A. Lepretre, *Nucl. Phys.* **A159**, 561 (1970).

<sup>9</sup>R. Pitthan, F. R. Buskirk, E. B. Dally, J. N. Dyer, and X. K. Maruyama, *Phys. Rev. Lett.* **33**, 849 (1974).

<sup>10</sup>Refined by International Nickel Corporation and designated INCO 200.

<sup>11</sup>Manufactured by Seforad-Applied Radiation Ltd.

<sup>12</sup>*Neutron Cross Sections*, compiled by J. R. Stehn, M. D. Goldberg, B. A. Magnuro, and R. Weiner-Chasman, Brookhaven National Laboratory Report No.

BNL-325 (NTIS, Springfield, Va., 1964).

<sup>13</sup>R. Batchelor and G. C. Morrison, *Fast Neutron Physics Part I* (Interscience, New York, 1960).

<sup>14</sup>J. M. Cuttler (private communication).

<sup>15</sup>K. W. Geiger and C. K. Hargrove, *Nucl. Phys.* **53**, 204 (1964).

<sup>16</sup>J. E. McFee, A. F. M. Ishaq, T. J. Kennett, and W. V. Prestwich, *Phys. Lett.* **55B**, 369 (1975).

<sup>17</sup>A. H. Wapstra and N. B. Grove, *Nucl. Data* **A9**, 265 (1971).

<sup>18</sup>M. R. Schmorak and R. L. Auble, *Nucl. Data* **B5**, 207 (1971).

<sup>19</sup>K. K. Seth, *Nucl. Data* **B7**, 161 (1972).

<sup>20</sup>J. H. Hamilton, V. Ananthkrishnan, A. V. Ramayya, W. M. LaCasse, D. C. Camp, J. J. Pinajian, L. H. Kern, and J. C. Manthuruthil, *Phys. Rev. C* **6**, 1265 (1972).

<sup>21</sup>M. A. Preston, *Physics of the Nucleus* (Addison-Wesley, Reading, Massachusetts, 1962).

<sup>22</sup>E. H. Auerbach and F. G. J. Perey, Brookhaven National Laboratory Report No. BNL-765, 1962 (unpublished).

<sup>23</sup>H. Lycklama, T. J. Kennett, and L. B. Hughes, *Can. J. Phys.* **47**, 666 (1969).

<sup>24</sup>C. D. Bowman, R. J. Baglan, and B. L. Berman, *Phys. Rev. Lett.* **23**, 796 (1969).

<sup>25</sup>K. K. Seth, *Nucl. Data* **A2**, 299 (1966).